

A CONCEPTUAL MODEL FOR GAS-LIQUID INTERACTION AND ITS INTEGRATION INTO CFD SIMULATION OF BUBBLE COLUMNS

Ning YANG*, Jianhua CHEN, Wei Ge and Jinghai LI

Institute of Process Engineering, Chinese Academy of Sciences, Beijing, 100190, P.R.CHINA
 *Corresponding author, E-mail address: nyang@home.ipe.ac.cn

ABSTRACT

Closure models for describing bubble-liquid interactions are challenging problems for the simulation of gas-liquid flow in bubble columns or slurry beds. This work extends the modelling strategy of Energy-Minimization Multi-Scale (EMMS) method originally proposed for gas-solid fluidization to the simulation of gas-liquid systems, leading to a Dual-Bubble-Size (DBS) model featuring the closure of a hydrodynamic model with a stability condition reflecting the compromise between different dominant mechanisms in the system. A conceptual analysis is thus performed on the momentum and energy transfer modes between phases. The model calculation captures a jump change on the curve of gas holdup vs. superficial gas velocity, which could be physically interpreted as a shift from the homogeneous and transition regimes to the heterogeneous regime. It is found that the jump change is due to the shift of the global minimum point of the micro-scale energy dissipation between two local minimum points in the 3D space of structure parameters. The competition between the small bubble and large bubble classes could be used to explain the dual effect of liquid viscosity and surface tension on the stability of homogeneous flow. Then a new drag model is extracted from the DBS model and integrated into the CFD simulation of a bubble column. Our preliminary study shows that the total gas hold-up curve and the radial gas hold-up profile can be reasonably predicted with the new drag model compared to the experiments in literature reports.

NOMENCLATURE

C_{Db}	drag coefficient for a bubble in a swarm
$C_{D0,b}$	drag coefficient for a bubble in a quiescent liquid
C_{Dp}	drag coefficient for a particle in a particle swarm
$C_{D0,p}$	drag coefficient for a particle in a quiescent fluid
c_f	coefficient of surface area increase
d_{crit}	critical bubble diameter
d_b	bubble diameter
d_L	bubble diameter of large bubbles
d_{min}	minimum bubble diameter
d_S	bubble diameter of small bubbles
Eo	Eötvös number
f_b	volume fraction of gas phase
f_L	volume fraction of large bubbles
f_S	volume fraction of small bubbles
f_{BV}	breakup ratio of daughter to its mother bubble
Mo	Morton number
N_{break}	energy consumption rate due to bubble breakage and coalescence per unit mass, m^2/s^3
N_{surf}	rate of energy dissipation due to bubble oscillation per unit mass, m^2/s^3

N_{turb}	rate of energy dissipation in turbulent liquid phase per unit mass, m^2/s^3
N_{st}	rate of energy dissipation for suspending and transporting particles per unit mass, m^2/s^3
N_T	total rate of energy dissipation
n_b	number density of bubbles, $1/m^3$
P_b	bubble breakup probability, dimensionless
U_g	superficial gas velocity, m/s
$U_{g,L}$	superficial gas velocity for large bubbles, m/s
$U_{g,S}$	superficial gas velocity for small bubbles, m/s
$U_{g,trans}$	transition gas velocity, m/s
U_l	superficial liquid velocity, m/s
W_{st}	rate of energy dissipation for suspending and transporting particles per unit volume, m^2/s^3

Greek letters

ε	voidage, dimensionless
λ	character size of eddy, m
μ	viscosity, Pa·s
ρ	density, kg/m^3
σ	surface tension, N/m
ω	collision frequency, $1/s$

Subscripts

g	gas
l	liquid
L	large bubble
p	particle
S	small bubble

INTRODUCTION

Bubble columns and slurry beds have found widespread applications in mineral, chemical, biochemical, environmental, pharmaceutical industries due to the advantage of easy construction, lower energy consumption and excellent mixing capability. However, the flow structure in these systems is very complicated not only in micro-scale behaviour of single bubbles such as bubble shape, bubble oscillation, bubble wake and path instability, but in macro-scale phenomena of global systems. For instance, three flow regimes, namely, homogeneous (bubbly), transition and heterogeneous, have been found in bubble columns. The homogeneous regime occurs at lower gas velocities, followed by a transition regime at intermediate gas velocities, and finally the heterogeneous regime appears at higher gas velocities. Liquid movement and bubble properties, e.g., liquid circulation, bubble size distribution and two-phase structures are quite different depending on various flow regimes, and the understanding of underlying physics is still not clear due to the complexity of these phenomena.

While a large number of experimental methods have been developed to investigate the regime transition in bubble columns, Computational fluid dynamics (CFD) has emerged as a powerful tool for simulating such systems in recent decade, thanks to the advancement of computer technology. A series of articles have reviewed the state of the art of the CFD modelling and simulation for bubble columns (Jakobsen, Sannæs, Grevskott, & Svendsen, 1997; Joshi, 2001, 2002; Oey, Mudde & van den Akker, 2003; Rafique, Chen, Duduković, 2004; Sokolichin, Eigenberger & Lapin, 2004; Monahan & Fox, 2007; among others). It is found that CFD simulation for bubble columns is strongly dependent on the closure models involving drag, lift and virtual mass forces and bubble-induced turbulence models. Even the grid resolution and discretization schemes for convection term may affect the simulation. There is still no general consensus on model formulation. This may be due to the fact that the terms reflecting gas-liquid interaction occurring at different scales are difficult, if not impossible, to be extracted or generalized from experimental measurements or micro-scale and direct numerical simulations.

The complexity of multi-scale structure has been explored via some variational criteria (Li & Kwauk, 1994). The basic idea is that the multi-scale structure resulting from the correlation between scales can be physically attributed to the compromise between dominant mechanisms which are mathematically expressed as various extremum tendencies (Ge, et al., 2007). The so-called stability condition can therefore be formulated by a mutually constrained extremum reflecting the compromise of mechanisms. This idea was first introduced in the modelling of gas-solid fluidization with the energy-minimization multi-scale (EMMS) model (Li & Kwauk, 1994). Following this strategy, we have attempted to extend the idea of scale differentiation and analysis of compromise of dominant mechanisms to gas-liquid systems. This article reviews our recent works in this topic and introduces some new preliminary results of CFD simulation (Yang, et al., 2007, 2009; Chen et al., 2009a, 2009b). For details, the interested reader can be referred to the aforementioned publications.

DESCRIPTION OF THE DBS MODEL

Partition of energy dissipation and stability condition

Figure 1 can be used to illustrate the mode of the momentum transfer and energy dissipation in bubble columns. Small bubbles resemble rigid particles and non-slip boundary condition can be imposed in direct numerical simulation, and drag coefficient of small bubbles approximates that of particles with same diameter (case A). With the increase of bubble size, the drag coefficient of bubbles begins to deviate from that of particles due to the slip of liquids along bubble surfaces (case B). Larger bubbles may change its shape or oscillate when undergoing strong interaction with bubble wake and liquid turbulence (case C). With further increase of bubble size and intensity of gas-liquid interaction, arriving eddies with characteristic length scale smaller than these bubbles whilst containing sufficient kinetic energy could induce the breakage of target bubbles (case D).

The total energy consumption per unit mass of liquid N_T can be derived from the rate of work done by the drag force on unit mass of liquid and reduced to

$$N_T = U_g g \quad (1)$$

for bubble columns. If the gas is fully composed of small bubbles, N_T is transferred from bubbles to liquid through shear stress and non-slip boundary, and then transferred and finally dissipated in the process of energy cascade of liquid turbulence (case A). But for other cases only a part of N_T is directly transferred from bubbles to liquid in this way, and the remaining part denoted by N_{surf} accounts for the energy consumption due to the slip of liquid along bubble surfaces and shape oscillation and can be formulated as

$$N_{\text{surf}} = \left[1 - \frac{C_{D,p}}{C_{D,b}} \right] N_T \quad (2)$$

though it is only a rough description of the complicated interphase energy exchange. The first part of N_T is also not completely dissipated via energy cascade and a portion of this may store temporarily as surface energy generated from bubble breakage N_{break} and finally dissipated in the process of bubble coalescence. This implies that no net surface is generated when the dynamic balance between breakup and coalescence is well established. N_{break} can be formulated as

$$N_{\text{break}} = \int_{\lambda_{\text{min}}}^{d_b} \int_0^{0.5} \frac{\omega(d_b, \lambda)}{(1-f_b)\rho_l + f_b\rho_g} \cdot P_b(d_b, \lambda, f_{BV}) \cdot c_f \pi d_b^2 \sigma \cdot df_{BV} d\lambda \quad (3)$$

where the arrival frequency $\omega(d_b, \lambda)$ and the breakage probability $P_b(d_b, \lambda, f_{BV})$ can be obtained from the classical statistical theory of isotropic turbulence. The total energy N_T was thus decomposed into three parts:

$$N_T = N_{\text{surf}} + N_{\text{turb}} + N_{\text{break}} \quad (4)$$

by Zhao (2006) and Ge, et al. (2007).

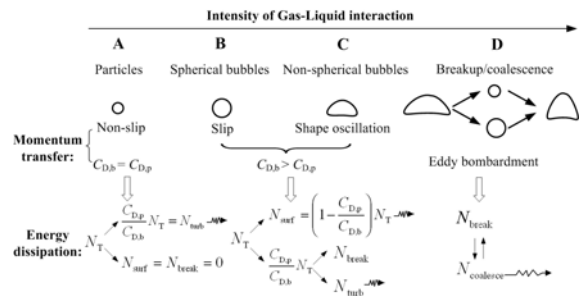


Figure 1: Mode of momentum transfer and energy dissipation between gas and liquid. (Yang et al., 2009)

Structure resolution and model equations

The bi-modal bubble size distribution and coexistence of small and large bubbles is well known for bubble columns. Thus Yang, et al. (2007) extended the Single-Bubble-Size (SBS) model of Zhao (2006) and Ge, et al. (2007) to a Dual-Bubble-Size (DBS) model so that the state of the system heterogeneity can be simply specified by several structure variables: bubble diameters (d_s, d_l), volume fraction (f_s, f_l) and superficial gas velocities ($U_{g,s}, U_{g,l}$). The liquid structure is assumed to be shared by the two bubble classes and therefore not resolved. The way of partition of energy dissipation can thus be extended to the system with two bubble classes. With the common circumstances of viscous dissipation N_{turb} , each bubble class dissipates energy via the slip of liquid along bubble surfaces and shape oscillation of bubbles ($N_{\text{surf},S}, N_{\text{surf},L}$).

Each bubble class breaks up and generates new surfaces by extracting energy from liquid turbulence ($N_{\text{break,S}}$, $N_{\text{break,L}}$) and finally dissipates in the course of bubbles coalescence which may occur between the bubbles belonging to same class or between different classes. Therefore the stability condition can be rewritten as the minimization of all of the micro-scale dissipation:

$$N_{\text{surf,S}} + N_{\text{surf,L}} + N_{\text{turb}} = \min \quad (5)$$

or the maximization of all of the meso-scale energy dissipation:

$$N_{\text{break,S}} + N_{\text{break,L}} = \max \quad (6)$$

Each energy dissipation term in Eqs. (5)-(6) is a function of structure parameters under a given superficial gas velocity, and hence the stability condition drives the evolution of system structure with gas velocity. The mass and force balance equations for the two bubble classes can be formulated as

$$f_i \rho_l g = \frac{f_i}{\pi/6 \cdot d_i^3} \cdot C_{D,i} \frac{\pi}{4} d_i^2 \cdot \frac{1}{2} \rho_l \left(\frac{U_{g,i}}{f_i} - \frac{U_l}{1-f_b} \right)^2 \quad (7)$$

$$\sum_i U_{g,i} = U_g \quad (8)$$

The subscript i refers to S and L which simply represent two different bubble classes because the same drag correlations are employed for the two bubble classes and we do not distinguish small and large bubble classes artificially in the model equations. The correlations of Grace, et al. (1976) were used to calculate the drag coefficient. With specified U_g , U_l and physical properties of gas and liquid for the system, Eqs. (7)-(8) can be solved to obtain the structure variables f_S , f_L and $U_{g,L}$ by giving the trial value for d_S , d_L and $U_{g,S}$. Then the stability condition, i.e., Eq. (6), is used to determine the set of the six structure variables corresponding to the minimum of the micro-scale energy dissipation.

RESULTS OF THE DBS MODELLING

Jump change and regime transition

The two points marking the regime transition according to Zahradnik, et al. (1997) can be reasonably predicted with the DBS model for air-water system, as shown in Fig. 2. The calculation is well consistent with the experiments of Camarasa, et al. (1999) for the case of multiple orifice nozzle for U_g less than 0.07 m/s covering the first point at which U_g equals 0.04m/s, and the dampening of the tendency of increasing gas holdup can be reflected in the calculation. Though the model fails to predict the S-shaped gradual variation in medium gas velocities, a jump change between 0.128 and 0.129 m/s of gas velocities can be captured, which is very close to the second regime transition point of Zahradnik, et al. (1997) and Camarasa, et al. (1999). Note that the model does not consider the effects of sparger types and column diameters which were report to play important role in flow structure and regime transition. In this sense, we expect that this conceptual model could reflect some intrinsic characteristics of gas-liquid flow and structure evolution of the system. Mudde et al. (2009) reported that the maximum point of gas holdup was more pronounced to form a summit and then a sharp drop can be observed when using needle spargers and contaminated tap water.

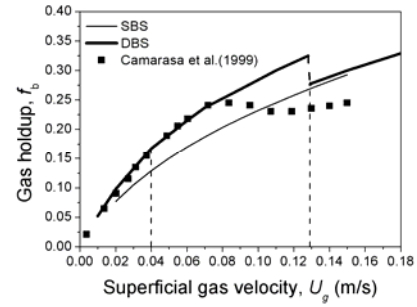


Figure 2: Model calculation of Yang et al. (2007) and experiments of Camarasa et al. (1999) with multiple orifice nozzle for air/water system.

Physical essence of the jump change

To ascertain the physical essence of the calculated jump change, the iso-surfaces of $N_{\text{surf}}+N_{\text{turb}}$ in the 3D space of structure parameters for the two gas velocities near the jump change is illustrated in Fig. 4. The minimum point jumps from one ellipsoid for 0.128 m/s of gas velocity to another for 0.129 m/s, causing the jump change of the diameter of small bubble from 1.42mm to 2.86mm. Thus it is the stability condition that drives the variation of structure parameters and hence the jump change.

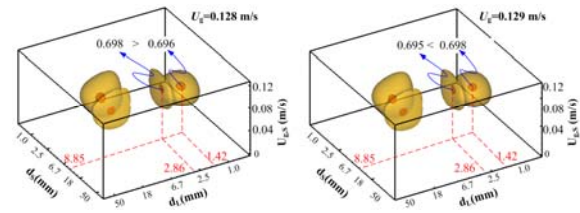


Figure 3: Model calculation of Yang et al. (2007) and experiments of Camarasa et al. (1999) with multiple orifice nozzle for air/water system.

Dual effect of liquid viscosity and surface tension

Ruzicka et al. (2003) reported that liquid viscosity has dual effects on regime transition: moderate viscosity (3-22 mPa·s) destabilizes the homogeneous regime and advances the transition, whereas low viscosity (1-3 mPa·s) stabilizes the homogeneous regime. Interestingly, this experimental finding could be reproduced by the calculation with the DBS model, as illustrated in Fig. 4.

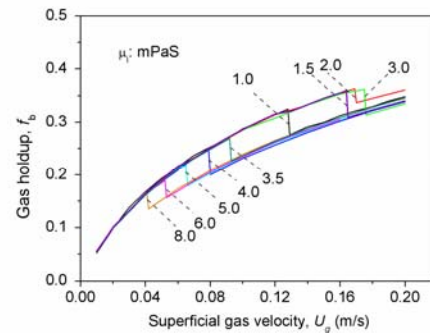


Figure 4: Gas holdup calculated from the DBS model for different liquid viscosities (Yang et al., 2009).

It can be observed that compared to air-water systems of 1.0 mPa·s of liquid viscosity, slight increase in liquid viscosity from 1.0 to 3.0 mPa·s delays the jump change to

higher gas velocities for air-glycerin solution systems, showing the stabilizing effect on homogeneous regime. Further increase of viscosity from 3.5 to 8.0 mPa-s advances the jump change to lower gas velocities, thereby implying the destabilization of the homogeneous regime.

Competition of the small and the large bubble classes

Fig. 5 shows that d_s increases and d_L decreases with increasing U_g for air-water systems. When jump change of total gas holdup occurs from 0.128 to 0.129 m/s of U_g , the structure parameters for large bubbles (d_L , f_L) change little, but d_s increases abruptly to a large value denoted by d_{crit} and the significant drop of f_s causes the larger decrease of total gas holdup. Beyond the U_g of jump change, d_s is invariable and d_L continues to decrease. We can define d_{crit} as the critical bubble diameter of the bubble class for which jump change occurs. We find that d_{crit} corresponds to the lowest point on the curve of drag coefficient as a function of bubble diameter, as illustrated in Fig. 6. Typically the minimum exists for almost all of drag coefficient correlations, marking the distinction of viscous- and surface tension-dominant regimes. But the relation of this minimum with jump change is rather complicated due to the non-linear coupling of the model equations and the stability condition.

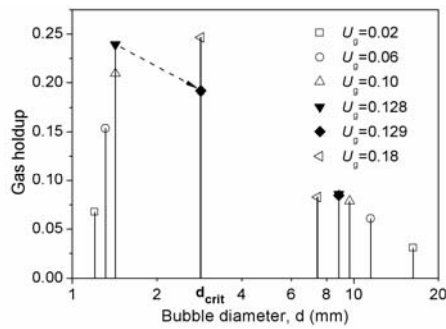


Figure 5: Gas holdup of the two bubble classes at different U_g (m/s) (air/water, Yang et al., 2007).

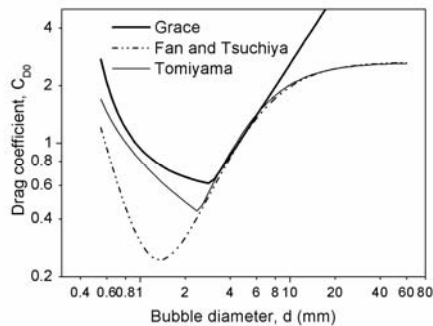


Figure 6: Different drag coefficient correlations

In contrast to air-water systems, Fig. 7 illustrates three different tendencies of structure parameters for different liquid viscosities of air-glycerin solution systems, showing that d_{crit} increases with the liquid viscosity. The diameter of small bubbles d_s increases and then jump to d_{crit} and the diameter of large bubbles d_L first decreases and then keep constant at the jump point for low viscosity (1.5 mPa-s, Fig. 7a); whereas this structure variation reverses at high viscosity (5.0 mPa-s, Fig. 7c), indicating that d_s varies little but d_L jumps to d_{crit} . Both d_s and d_L jump to d_{crit} at the medium viscosity (3.0 mPa-s, Fig. 7b). The two bubble

classes seem to compete with each other to jump to a stable state with bubble diameter being d_{crit} . But at low viscosity, only the diameter of small bubbles could reach d_{crit} ; whereas at high viscosity, large bubbles have the priority to reach d_{crit} . It can be concluded that the homogeneous flow can keep its stability even at higher gas velocity when the small bubble diameter d_s jumps to d_{crit} first, but lose its stability at lower gas velocity if the large bubble diameter d_L first achieves d_{crit} . This may offer a physical explanation for the dual effect of liquid viscosity. Surface tension is also found to have the dual effect with this model calculation. The detail discussion is presented in our recent publication (Chen et al., 2009a; Yang et al., 2009).

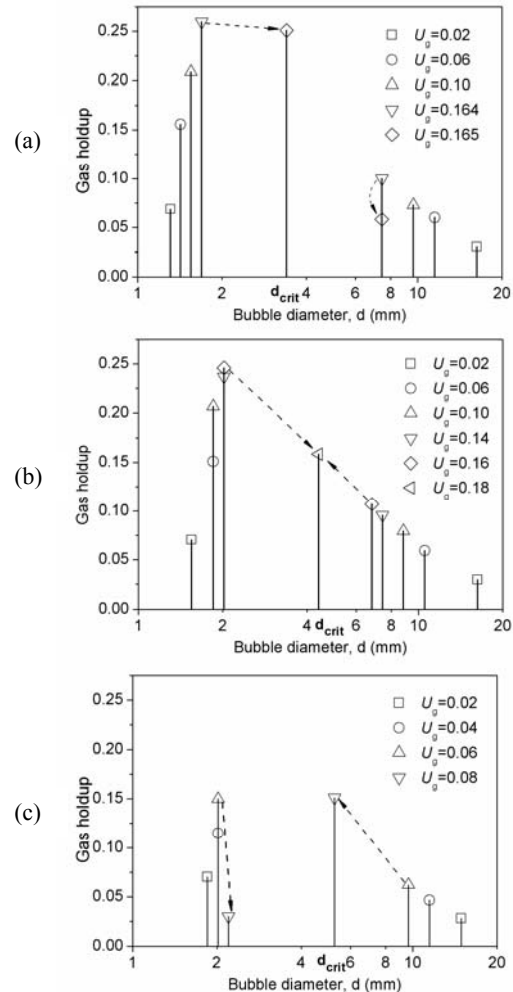


Figure 7: Gas holdup of the two bubble classes and variation of bubble diameter for different liquid viscosities (a) 1.5mPaS (b) 3.0mPaS (c) 5.0mPaS (Yang et al., 2009)

Similarity between gas-solid and gas-liquid systems

Li et al. (1999) reported a bifurcation phenomenon for gas-solid fluidization with the EMMS model calculation, indicating that the so-called choking can be captured through the bifurcation of different energy dissipation terms. This finding can also have its counterpart in gas-liquid systems, as reported in detail in Chen et al. (2009b), reflecting the compromise between two dominant mechanisms. Each branch causing the bifurcation may represent a candidate of stable state, and the switch from one to the other signifies the fundamental variation of system structure leading to regime transition.

INTEGRATION WITH CFD SIMULATION

Formulation of a new drag model

Drag force is reported to play significant role in CFD simulation and often formulated as below:

$$\mathbf{F}_g^D = \frac{3}{4} \alpha_g \rho_l \frac{C_D}{d_b} |\mathbf{u}_l - \mathbf{u}_g| (\mathbf{u}_l - \mathbf{u}_g) \quad (9)$$

C_D/d_b proves to be a key parameter for simulation, and usually calculated from some correlations with specified bubble diameter or even assumed as constant for some cases. In this work, we can extract a formulation for C_D/d_b from the DBS model, as shown below.

$$\frac{C_D}{d_b} = \left[\frac{f_s}{d_s} \cdot C_{D,s} \left(\frac{U_{g,s}}{f_s} \right)^2 + \frac{f_L}{d_L} \cdot C_{D,L} \left(\frac{U_{g,L}}{f_L} \right)^2 \right] \frac{f_b}{U_g^2} \quad (10)$$

It can be seen that C_D/d_b is a function of superficial gas velocity and structural parameters. Fig. 8 shows the calculated C_D/d_b with the DBS model.

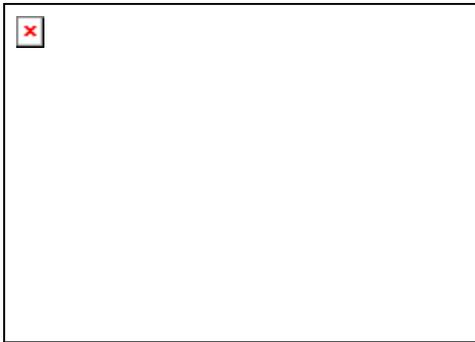


Figure 8: Ratio of drag coefficient to bubble diameter obtained from the DBS model. (Chen et al., 2009b)

CFD simulation of a bubble column

The conservative equations for gas and liquid can be written as

$$\frac{\partial \alpha_k}{\partial t} + \nabla \cdot (\alpha_k \mathbf{u}_k) = 0 \quad (11)$$

$$\frac{\partial \alpha_k \rho_k \mathbf{u}_k}{\partial t} + \nabla \cdot (\alpha_k \rho_k \mathbf{u}_k \mathbf{u}_k) = -\alpha_k \nabla P + \alpha_k \rho_k \mathbf{g} \pm \mathbf{F}_{kl} + \nabla \cdot (\alpha_k \boldsymbol{\tau}_k) + \nabla \cdot (\alpha_k \rho_k \mathbf{u}_k' \mathbf{u}_k') \quad (12)$$

The CFD simulation was carried out for the bubble column of Camarasa et al. (1999) with an inside diameter of 10cm and a height of 2m in which three kinds of spargers, named single-orifice, multiple-orifice and porous plate were used. In this work, 3D unsteady simulation are performed with the commercial CFD software Fluent 6.3. Four gas velocities, i.e. 2.03, 3.72, 6.06, 7.22 cm/s are simulated with two boundary conditions for the top outlet. The radial gas hold-up are compared with the experimental data of porous plate. The freeboard above the gas-liquid dispersion may cause some convergence problem, as discussed by Ranade (1997). Therefore a degassing boundary condition is used for the top surface. Another substitute to eliminate the effects of freeboard is the using of pressure-outlet boundary condition in conjunction with the column filled by gas-liquid dispersion, which is ensured by liquid backflow. For this reason, the 3D simulation only has a height of 1.5m, the mesh length scale is 0.005 m at the circumference and 0.01 m in the axial direction.

For all cases standard k-ε mixture model is used and the wall is no-slip for liquid phase and free-slip for gas phase.

Eq. (10) is used to calculate the drag force. The discretization scheme is first order upwind and time step is fixed as 0.01s.

Figure 9 and Figure 10 respectively show the calculation of total and radial gas hold-up for Degassing-BC cases. It can be seen that the radial gas hold-up for $U_g=6.06$ cm/s and $U_g=7.22$ cm/s agree with experimental data quite well. But for lower gas velocities discrepancy occurs between simulation and experiment. The simulated total gas hold-up is not satisfied when the Degassing-BC is used.

When the Pressure-BC is used, total gas hold-up are consistent with the multiple-orifice data for all of the four gas velocity cases, as shown in Figure 11. For the radial gas hold-up distribution, the Pressure-BC gives reasonable prediction for all gas velocities, as seen in Figure 12. The slightly flat profile for high gas velocities near the wall region may need further investigation.

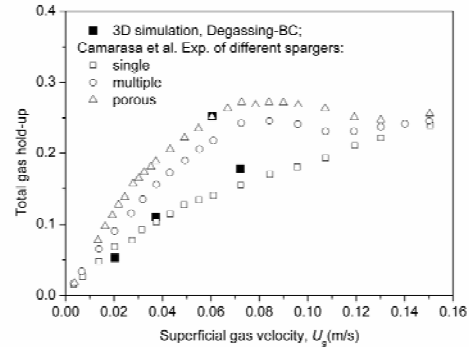


Figure 9: Comparison of total gas hold-up for the Degassing-BC cases.

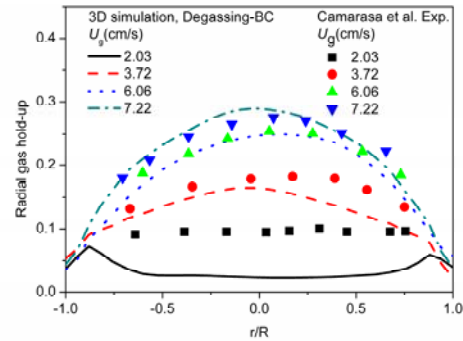


Figure 10: Comparison of radial gas hold-up for the Degassing-BC cases.

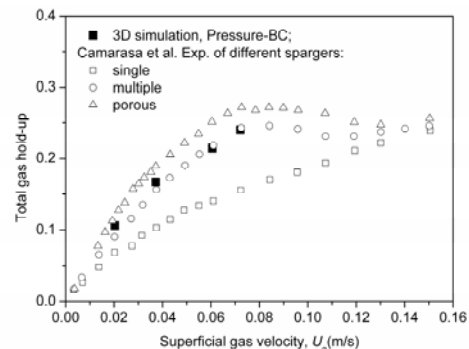


Figure 11: Comparison of total gas hold-up for the Pressure-BC cases.

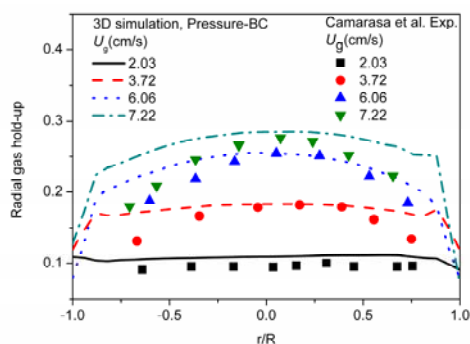


Figure 12: Comparison of radial gas hold-up for the Pressure-BC cases.

CONCLUSION AND PROSPECTS

The second regime transition point can be captured as a jump change of gas hold-up by the Dual-Bubble-Size (DBS) model. Physically this can be understood through the bifurcation of micro-scale energy dissipation between two branches, and the switch of the global minimum point of the micro-scale energy dissipation between two local minimum points in the 3D space of structure parameters. The bifurcation first explored in the EMMS model of our previous work to predict the so-called choking in gas-solid fluidization can also find its counterpart in gas-liquid systems in this work. Each branch may represent a candidate of stable state, and the switch from one to the other signifies the fundamental variation of system structure leading to the regime transition. The dual effect of liquid viscosity on flow stability can be reasonably predicted and interpreted from the perspective of the competition between the small bubble and the large bubble classes. Based on this strategy, the momentum transfer and energy dissipation in gas-liquid system is analysed. The ratio of drag coefficient to the bubble diameter C_D/d_b is of critical importance for CFD simulation and can be extracted from the DBS model calculation. CFD simulation incorporating the DBS drag model for interphase coupling can reasonably predict the total gas hold-up curve and the radial gas hold-up profile compared to the experiments in literature reports. Though this study is at its preliminary stage, it would be promising to further develop models following this modelling strategy for complex gas-liquid systems with improved accuracy and reveal some underlying physics for CFD simulation in the near future.

ACKNOWLEDGEMENT

The authors would like to thank the support from National Basic Research Program of China under the grant 2009CB219906.

REFERENCES

CAMARASA, E., VIAL, C., PONCIN, S., WILD, G., MIDOUX, N. and BOUILLARD, J., (1999), "Influence of coalescence behaviour of the liquid and of gas sparging on hydrodynamics and bubble characteristics in a bubble column", *Chem. Eng. Process.*, 38, 329-344.

CHEN, J., YANG, N., GE, W. and LI, J., (2009a), "Modeling of regime transition in bubble columns with stability condition", *Ind. Eng. Chem. Res.*, 48, 290-301.

CHEN, J., YANG, N., GE, W. and LI, J., (2009b), "Computational fluid dynamics simulation of regime transition in bubble columns incorporating the Dual-Bubble-Size model", *Ind. Eng. Chem. Res.*, 48, 8172-8179.

GE, W., CHEN, F., GAO, J., GAO, S., HUANG, J., LIU, X., REN, Y., SUN, Q., WANG, L., WANG, W., YANG, N., ZHANG, J., ZHAO, H., ZHOU, G., LI, J., (2007), "Analytical multi-scale method for multi-phase complex systems in process engineering — Bridging reductionism and holism", *Chem. Eng. Sci.*, 62, 3346-3377.

GRACE, J. R., WAIREGI, T., NGUYEN, T. H., (1976), "Shapes and velocities of single drops and bubbles moving freely through immiscible liquids", *Trans. IChemE*, 54, 167-173.

JAKOBSEN, H. A., SANNÆS, B. H., GREVSKOTT, S., SVENDSEN, H. F., (1997), "Modeling of Vertical Bubble-Driven Flows", *Ind. Eng. Chem. Res.* 36, 4052-4074.

JOSHI, J. B., (2001), "Computational flow modelling and design of bubble column reactors", *Chem. Eng. Sci.*, 56, 5893-5933.

LI, J., KWAIK, M., (1994), "Particle-Fluid Two-Phase Flow—The Energy-Minimization Multi-Scale Method", Metallurgical Industry Press, Beijing.

MONAHAN, S. M., FOX, R. O., (2007), "Effect of Model Formulation on Flow-Regime Predictions for Bubble Columns", *AIChE J.*, 53, 9-18.

OEY, R. S., MUDDE, R. F. and VAN DEN AKKER, H. E. A., (2003), "Sensitivity study on interfacial closure laws in two-fluid bubbly flow simulations", *AIChE J.*, 49, 1621-1636.

RAFIQUE, M., CHEN, P., DUDUKOVIC, M. P., (2004), "Computational Modeling of Gas-liquid Flow in Bubbling Columns", *Rev. Chem. Eng.*, 20, 225-375.

RANADE, V. V., (2002), "Computational Flow Modeling for Chemical Reactor Engineering", Academic Press, New York.

RUZICKA, M. C., DRAHOS, J., MENA, P. C., TEIXEIRA, J. A., (2003), "Effect of viscosity on homogeneous-heterogeneous flow regime transition in bubble columns", *Chem. Eng. J.*, 96, 15-22.

SOKOLICHIN, A., EIGENBERGER, G. and LAPIN, A., (2004), "Simulation of buoyancy driven bubbly flow: established simplifications and open questions", *AIChE J.*, 50(1), 24-45.

YANG, N., CHEN, J., GE, W. and LI, J., (2007), "Explorations on the multi-scale flow structure and stability condition in bubble columns", *Chem. Eng. Sci.*, 62, 6978-6991.

YANG, N., CHEN, J., GE, W. and LI, J., (2009), "A conceptual model for analyzing the stability condition and regime transition in bubble columns", *Chem. Eng. Sci.*, doi:10.1016/j.ces.2009.06.014.

ZAHRADNIK, J., FIALOVA, M., RUZICKA, M., DRAHOS, J., KASTANEK, F., THOMAS, N. H., (1997), "Duality of the gas-liquid flow regimes in bubble column reactors", *Chem. Eng. Sci.*, 52, 3811-3826.

ZHAO, H., (2006), "Multi-scale modeling of gas-liquid (slurry) reactors", Ph.D. Thesis, Institute of Process Engineering, Chinese Academy of Sciences, Beijing.